PHOTOMASK

BACUS—The international technical group of SPIE dedicated to the advancement of photomask technology.

BACUS N • E • W • S

AUGUST 2014
VOLUME 30, ISSUE 8

Best Paper - EMLC14

Contact Hole Multiplication using Grapho-Epitaxy Directed Self-Assembly: Process Choices, Template Optimization, and Placement Accuracy

Joost Bekaert, Roel Gronheid, Boon Teik Chan, and Geert Vandenberghe, imec, Kapeldreef 75, B-3001 Leuven, Belgium

Jan Doise and Vijaya-Kumar Murugesan Kuppuswamy, imec, Kapeldreef 75, B-3001 Leuven, Belgium and Katholieke Universiteit Leuven, Department of Electrical Engineering (ESAT), Kasteelpark Arenberg 10, B-3001, Leuven, Belgium

Yi Cao and YoungJun Her, AZ Electronic Materials, 70 Meister Avenue, Branchburg, NJ 08876, USA

ABSTRACT

Directed Self Assembly (DSA) of Block Co-Polymers (BCP) has become an intense field of study as a potential patterning solution for future generation devices. The most critical challenges that need to be understood and controlled include pattern placement accuracy, achieving low defectivity in DSA patterns and how to implement this process as a patterning solution. The DSA program at imec includes efforts on these three major topics.

Specifically, in this paper the progress for the templated DSA flow within the imec program will be discussed. An experimental assessment is made based on a 37 nm BCP pitch material. In particular, the impact of different process options is illustrated, and data for CD and placement accuracy of the DSA holes in their template is provided.

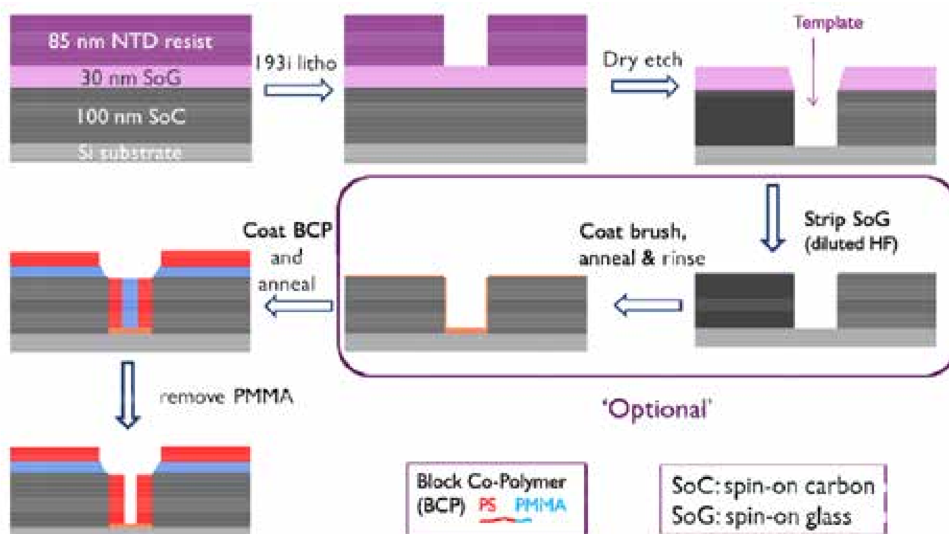

Figure 1. Schematic representation of the template DSA flow as implemented at imec.

TAKE A LOOK INSIDE:

INDUSTRY BRIEFS
—see page 10

CALENDAR
For a list of meetings
—see page 11

SPIE.

9231-21

Editorial

The "European Mask and Lithography Conference", EMLC is in its 30th year.

Uwe Behringer, UBC Microelectronics, Germany, EMLC2014 Conference Chair

The 30th European Mask and Lithography Conference, EMLC 2014 was held on June 24th and June 25th, 2014 at the Hilton Hotel, Dresden, Germany. The conference, which has brought together 160 scientists, researchers, engineers, and technologists, provided an overview of the mask status and future strategy. This year's sessions included papers on: "Mask Writing Time Optimization"; "EUV Lithography"; "EUV Mask Technology"; "E-Beam Technologies"; "Templates Technologies"; "Simulation"; "Metrology"; "Wafer Processing"; "DSA Technology and alternative Lithography" and "Processes and Special Technologies".

As Welcome Speaker, Heinz Martin Esser, CEO Roth & Rau – Ortner GmbH, Dresden, introduced European's largest Cluster in the ICT (Information & Communication Technology). He described the efforts to build up a strong European cooperation beginning with a partnership with Grenoble (Minalogic) and extended to other European High-Tech Clusters (Silicon Europa) to establish a new European Identity in the global competition.

Our first keynote speaker, Jan Hendrik Peters from Carl Zeiss, SMS GmbH, Jena, Germany, talked about "EUV Mask Infrastructure – Are we ready to meet the demands for the consumer electronics market?" The second keynote speaker, Stefan Wurm from SEMATECH discussed the EUV Lithography-Process, challenges and outlook.

As a tradition, we invited the Best Paper of PMJ 2014 and the Best Poster from Photomask 2013: (Keisuke Yagawa-san from Toshiba Corp, "High Performance mask Fabrication Process for Next-Generation Mask Production" and Natalia Davydova et al. from ASML, "Black Border, Mask 3D Effects: covering Challenges of EUV Mask architecture for 22nm node and beyond"). We also invited S. Wurm from SEMATECH to present information regarding the 12th Annual Mask Industry Survey.

Best Paper of EMLC2014

From the 160 conference attendees we got 112 evaluation sheets back, so it was easy to select the Best Paper of the EMLC2014, by Joost Bekaert et al from IMEC, "Contact Hole Multiplication using Grapho-Eptaxy Directed Self Assembling : Process Choices, Template Optimization and Placement Accuracy".

What did we learn from the EMLC2014?

- 12th annual mask industry survey: All nine participating mask shops shipped masks targeted for ≤22 nm with Yields > 90%. In 2013, about 45% of masks are ≥ 250 nm, and only 1%, between <22 nm and ≥ 16 nm.

The number of masks per set showed growth rate ~14% per node and has tripled since 250nm, with an increasing variation for high end products. Glass size and type: More than 88% are 6" and 86% are binary masks. The Mask Market was about $3 billion against the Semiconductor Market of about $ 300 billion and the Consumer Electronic Market of $750 billion.

- Mask writing time: Paul Ackmann from Globalfoundries showed how reticle write time increased node-to-node. The cost of mask sets was increasing too, driven by the tighter requirements, more levels, and higher capital investment. New patterning tools with improved performance were unable to compensate for the increased data and complexity. As a result, the writing time of a reticle for the 40 nm node was 10 hours, but for the 28 nm node, it increased to 28 hours on the same tool.
- EUV Technology: In 2014, the EUV source of 70 W allowed to expose 52 eight-inch wafers per hour. The ASML /Cymer roadmap predicts 125 wafer / hr in 2015 on a 250 W source. Critical issues included substrate quality, defect free deposition, substrate/blank cleans and blank inspection. The substrate surface still shows high variability. CMP and cleaning damage is hard to control on ULE and LTEM substrates. Less aggressive fine polishing techniques, such as Dressed Photon Nano-Polishing (DPNP), are required. Important is also the problem to keep the mask clean. ASML is working on a pellicle technology using a 70nm poly-silicon foil.

continues on page 9

N • E • W • S

BACUS News is published monthly by SPIE for BACUS, the international technical group of SPIE dedicated to the advancement of photomask technology.

Managing Editor/Graphics Linda DeLano
Advertising Lara Miles
BACUS Technical Group Manager Pat Wight

■ **2014 BACUS Steering Committee** ■

President
Frank E. Abboud, *Intel Corp.*

Vice-President
Paul W. Ackmann, *GLOBALFOUNDRIES Inc.*

Secretary
Bryan S. Kasprowicz, *Photronics, Inc.*

Newsletter Editor
Artur Balasinski, *Cypress Semiconductor Corp.*

2014 Annual Photomask Conference Chairs
Paul W. Ackmann, *GLOBALFOUNDRIES Inc.*
Naoya Hayashi, *Dai Nippon Printing Co., Ltd.*

International Chair
Uwe F. W. Behringer, *UBC Microelectronics*

Education Chair
Artur Balasinski, *Cypress Semiconductor Corp.*

Members at Large
Paul C. Allen, *Toppan Photomasks, Inc.*
Michael D. Archuletta, *RAVE LLC*
Peter D. Buck, *Mentor Graphics Corp.*
Brian Cha, *Samsung*
Glenn R. Dickey, *Shin-Etsu MicroSi, Inc.*
Brian J. Grenon, *Grenon Consulting*
Thomas B. Faure, *IBM Corp.*
Jon Haines, *Micron Technology Inc.*
Mark T. Jee, *HOYA Corp, USA*
Oliver Kienzle, *Carl Zeiss SMS GmbH*
Patrick M. Martin, *Applied Materials, Inc.*
M. Warren Montgomery, *The College of Nanoscale Science and Engineering (CNSE)*
Wilbert Odisho, *KLA-Tencor Corp.*
Michael T. Postek, *National Institute of Standards and Technology*
Abbas Rastegar, *SEMATECH North*
Emmanuel Rausa, *Plasma-Therm LLC.*
Douglas J. Resnick, *Canon Nanotechnologies, Inc.*
Thomas Struck, *Infineon Technologies AG*
Bala Thumma, *Synopsys, Inc.*
Jacek K. Tyminski, *Nikon Research Corp. of America (NRCA)*
Jim N. Wiley, *ASML US, Inc.*
Larry S. Zurbrick, *Agilent Technologies, Inc.*

SPIE.

P.O. Box 10, Bellingham, WA 98227-0010 USA
Tel: +1 360 676 3290
Fax: +1 360 647 1445
www.SPIE.org
help@spie.org

©2014

All rights reserved.

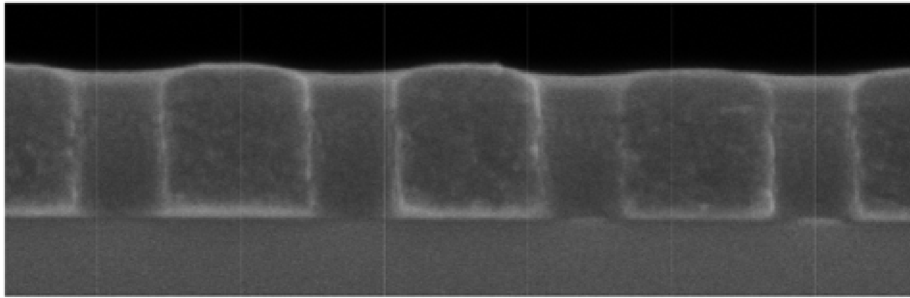

Figure 2. Cross-sectional image of a DSA template after etch, before applying BCP material. Straight sidewalls are obtained into the SoC layer.

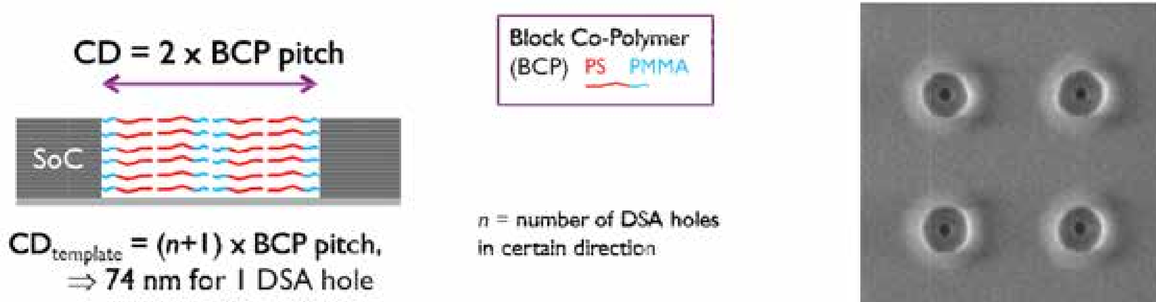

Figure 3. Left: Schematic representation of our current process, with PMMA-wetting SoC sidewalls and PMMA cylinder formation. Right: Top-down SEM image of singlet DSA holes formed within 74 nm CD tempates, after PMMA plug removal.

1. Introduction

Templated Directed Self Assembly (DSA) is a grapho-epitaxy process flow, in which a larger trench-like prepattern is printed by conventional lithography. In the confined space that is thus defined, a cylindrical phase Block Co-Polymer (BCP) material is allowed to phase separate which results in sub-resolution hole patterns. The number of holes that is obtained within each prepattern shape depends on the shape and size of the prepattern and the natural periodicity of the BCP material.

Templated DSA is mainly considered for application in via and/or cut mask levels. It is one of the most active areas of investigation within the field of DSA, because of its relatively feasible path for implementation with existing design flows, and the potential to replace a multiple patterning solution.[1] The gap between lithography scanner resolution and IC needs resulted in pitch division introduction starting with 22 nm MPU products. As the gap continues to grow, more pitch division/multiple exposures per layer will be needed in expense of edge placement errors, increasing tool and production costs. In this regard, templated DSA, as part of complimentary lithography, offers the possibility of providing large reduction of cost and processing time, by eliminating multiple via[2] or cut[3] masks.

In order to implement this approach for device fabrication, several outstanding processing-related issues need to be resolved. In this paper, we introduce the process for templated DSA that has been implemented at imec, using a 37 nm center-to-center BCP material. We discuss process options related to the prepattern optimization, and investigate the impact of local pattern density and BCP film thickness. Finally, experimental data is provided for the correlation of the DSA hole CD to the prepattern size, and for DSA hole placement accuracy within its prepattern.

2. Process Flow for Templated DSA Holes: Choices and Optimization

2.1 Overview of the basic steps and used materials

The grapho-epitaxy flow for DSA hole patterning with cylindrical phase BCP is schematically depicted in Figure 1.

A silicon substrate wafer is coated on a Sokudo DUO coat and development system, applying a typical tri-layer stack consisting of 100 nm spin-on carbon (SoC, HM710 from JSR Micro). On top of that, a negative tone development resist is coated (AN02 from FujiFilm). To define the prepattern templates in the resist, 193 immersion litho exposures were carried out on an ASML NXT:1950Gi scanner.

Next, the templates are etched into the SoC/SoG stack, using the TEL Tactras™ platform at imec. During the SoC etch all resist material is removed. A cross-section SEM image of a thus obtained template is shown in Figure 2. The resulting template is shown to be well-defined and have very straight sidewalls.

Now, the template is in principle ready for BCP application. However, a process choice may be to strip the SoG layer by means of diluted HF and/or apply a brush layer to the template (see further in section 2.4). As the final process step, the BCP is coated, typically resulting in partially conformal coating of the template topography. Annealing of the BCP results in phase separation of the blocks and forms the desired cylindrical hole patterns. Our current BCP process uses poly(styrene-block-methyl methacrylate) (PS-*b*-PMMA, AZEMBLY™ PME-585) with center-to-center

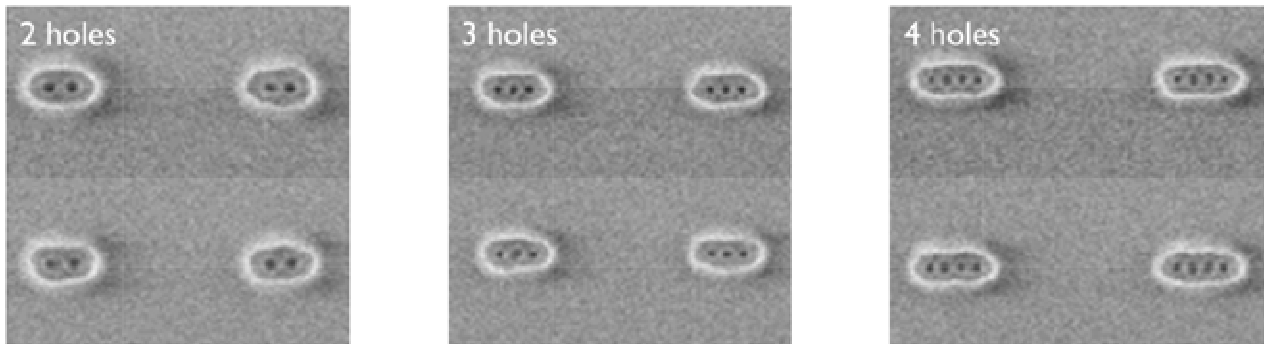

Figure 4. Top-down SEM images of short trenches with lengths commensurate with our 37 nm center-to-center distance BCP material, forming respectively 2, 3, and 4 DSA holes within the template.

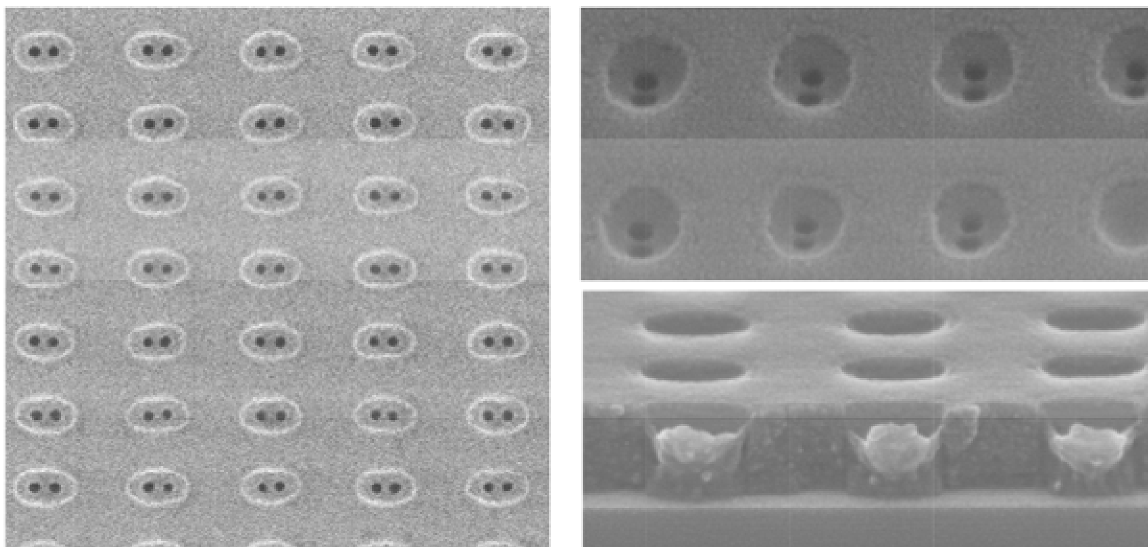

Figure 5. Top-down (left) and cross-sectional (right) images of short trenches filled with 37 nm center-to-center distance BCP material. We note recess of the BCP height within the template, and that the PS detaches from the surface.

distance = 37.1 nm, from AZ Electronic Materials. The BCP coat, anneal and development steps were processed off-line on a Tokyo Electron CLEAN TRACK ACT™ 12. A schematic representation of the cylindrical phase in our current process is shown in Figure 3. The SoC sidewalls are PMMA-wetting, and PMMA cylinders are formed in the templates. The minority block (in our case PMMA) is removed to form the DSA hole pattern. In our flow we use a wet development process for this PMMA removal. Wafers were analyzed using Hitachi CG4000/5000 top-down CD SEMs.

Besides singlet DSA holes as in Figure 3, also doublet DSA hole structures can be reliably obtained (Figure 4), when short trenches of appropriate dimensions (~74 nm by 111 nm) are filled with BCP material. Similarly, also more complex patterns can be generated with this process. Increasing the width of the trench, while keeping the height constant allows to selectively put 3, 4 or 5 holes in a trench. Not only linear patterns can be made, but also other shapes are feasible.[5]

2.2 3D Assessment

The tilted cross-section view top-right in Figure 5 demonstrates that the BCP material is not completely filling the template. Even the closed hole pattern at the far right of this image is not completely filling the template. Part of this underfilling may be a consequence of the wet development process that could results in some material shrinkage or loss. Through cross-section we would also like to get insight in the profile of the small holes that have been defined by the DSA process. Unfortunately, this has so far not been possible. When cleaving through the trenches, the polystyrene material itself is not cleaved and remains in one piece. This results in either empty trenches (if the PS is pulled out of the template by the cleaving) or a side view of the bowl-shaped PS material (as in Figure 5).

2.3 Pattern density effects

For more in-depth studies of the template hole process we have selected to work with the 2-hole patterns as shown in Figure 5. From a processing perspective we are interested to understand how patter density impacts the DSA process. Pattern density is expected to impact, since BCP material is needed to fill up the hole. In a dense pattern area, locally more material will be needed,

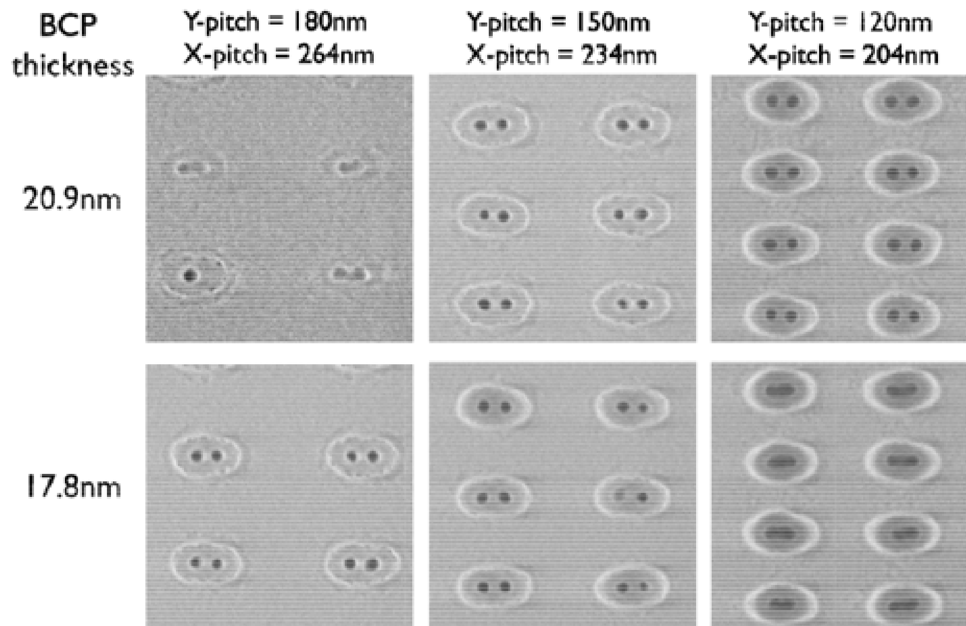

Figure 6. Top down SEM images of doublet DSA holes in short trenches at low (left), medium (middle) and high (right) pattern density for two different applied BCP film thicknesses. A clear impact of pattern density and BCP thickness is seen on the DSA hole information.

otherwise there will be underfilling of the holes. On the other hand, in more sparse regions overfilling of the template trenches may occur. The optical BCP film thickness is thus expected to depend on pattern density (among other things). This is indeed also observed experimentally (Figure 6). Short trenches (mask CD in Y-direction: 60 nm; in X-direction: 144 nm) are available at varying pattern density in our test structures. The pitch of the trenches is varied simultaneously in X and Y direction. The quoted BCP film thicknesses refer to the coating thickness on a flat silicon wafer. At the thickest BCP film thickness (20.9 nm) the target 2-hole patterns are properly formed for the medium and the high pattern density structures. The high density structure is slightly darker compared to the medium density case, which is indicative of slight underfilling. The low density structure at this film thickness however completely overfills and the target hole patterns are not opened. At lower film thickness (17.8 nm) the structures are properly formed in both the low and medium density case, but the medium density case is slightly darker because of underfilling. In this case the high density pattern is excessively underfilled resulting in merging of the two-hole patters. For a given film thickness there is therefore a window of pattern density that gives the desired DSA performance. Too high or too low density results in underfilling and overfilling, respectively.

2.4 SoG removal, brush application, and surface energy consideration

In the section above, it was demonstrated how the density and BCP thickness have an impact on the DSA hole formation. In addition, we see a clear sensitivity to process choice. As was mentioned in section 2.1, it is an option to remove the SoG layer by means of diluted HF after the template etch. When doing so, the BCP materials flows over the HF-rinsed SoC surface, instead of over the SoG surface. Since these have different surface energies, and hence a different affinity to the PMMA/PS components of the BCP, the result after annealing and DSA hole formation will be different. This can be seen in Figure 7 below, comparing the left versus the middle images (mask CD 120 nm/60 nm, pitch 180 nm/120 nm, and BCP coated thickness of 17.8 nm). DSA holes are formed at the center of the array for both the flow with and without SoG strip. This is because our BCP material shows a stronger flow over the SoC surface.

After the template etch, the template sidewalls are PMMA-wetting, which stimulates the cylindrical phase formation. However, also the template bottom is found to be PMMA-wetting. As a result, we may expect a thin residual layer of BCP material at the bottom of the template, preventing the DSA hole to be open all the way down to the bottom. This is represented by the modeled image at the left in Figure 8 (cfr. Reference [6]). The goal of applying a brush layer is to modify the surface energy at the bottom of the template such that it becomes neutral, meaning without preference to either PMMA or PS. In this case, the DSA hole should be better defined towards the substrate underneath. By doing so, however, the sidewall is expected to lose some of its PMMA-wetting strength. For illustration, the result of applying a brush (AZEMBLY™ NLD-244) is shown on the right hand side of Figure 7. As a side effect, the brush application is found to have a healing effect on the overfilling of the templates towards the array edge.

Clearly, the surface energies play a key role in the DSA formation, and work is in progress to understand the effects and how they can be applied for better DSA hole fidelity.

3. CD and Placement Accuracy for DSA Holes

3.1 Correlation of DSA hole CD to template CD

We investigated the dependency of the CD of the DSA hole on the template CD. In this study, we first considered simple single DSA holes with in a circular template (see Figure 9). On mask, the pattern is an array of square contacts (mask CD = 100 nm, 1X) on a regular

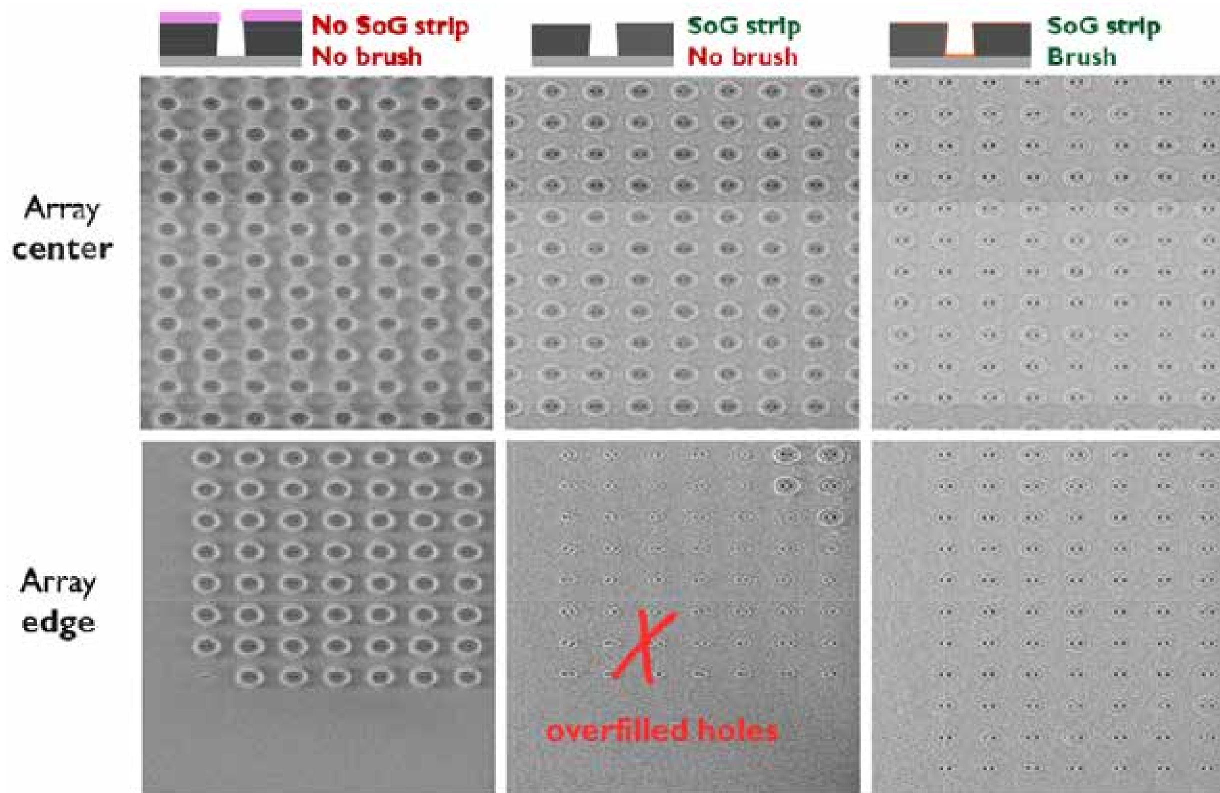

Figure 7. Illustration of the impact of process choice (SoG removal and brush layer application) on the DSA result.

square pitch of 200 nm. After litho, the top-down measured CD is in the order of 75 nm. After etch, this CD is about 70 nm when measured on the SoG surface (SoG was not stripped for this study on single holes). We know that the CD in the SoC, hence below the SoG top layer, measures slightly larger again around 74 nm.

After application of DSA, as in the right image of Figure 9 above, the CD of the template can still be measured. We found that this template CD 'after DSA' correlates very well with the template 'before DSA' (i.e. measured directly after etch), though with a process-dependent offset in the order of 1 nm not shown). As measurements were performed on a Focus-Exposure-Matrix (FEM) wafer, we could obtain the Bossung curve of the template CD as shown in Figure 10A.

When measuring the CD of the DSA hole within the exact same images, for the same dose and focus conditions, we obtain the graph in figure 10B. Figures 10 A and B clearly show how the Bossung of the template (with CDs around 70 nm) directly translates into a Bossung of the DSA holes (with CDs around 17 nm).

Indeed, when we make a correlation graph of the DSA CD versus the template CD, as in Figure 10C, we see how stretching/compressing the template around its optimum size leads to linear increase/decrease of the DSA hole CD. Of course, the stretching and compression of the template has limits: the blue points in graph C all correspond to features in which the DSA holes show an excellent open hole rate of practically 100% (at least seen from the top), while at template CDs below 62 nm or above 76 nm failures appear in the formation of the DSA holes.

With 4 individuals features per SEM image, and having captured 12 different SEM images at 1.2 µm separation, the points in the graphs A, B, and C are the average of 48 individual CDs. At best focus, we determined a typical 3σ variation on the CDs, and found 3σ = 3.4 nm on the template CD (slightly reduced to 3.1 nm after subtracting measured mask and metrology contributions). For the DSA CDs, we found 3σ = 2.5 nm (slightly reduced to 2.4 nm after subtracting the contribution of the template size dependency). This is illustrated in Figure 10D. Although we expect further improvements in the DSA hole CDU number, we can already note that the DSA hole CDU is better than the template CDU, which obviously is good.

3.2 Placement Accuracy Measurements

Having the images of the DSA holes within their templates at hand, we could determine the placement accuracy for these single DSA holes. To this end, we used the Hitachi High Technologies RED algorithm (Robust Edge Detection). This algorithm provides the coordinates of the center (of gravity) for both the template and the DSA hole. The (X,Y) delta between these centers is a measure for the displacement of the DSA hole within its template. Figure 11 shows the distribution of these placements errors. In the graph, the different colors correspond to different exposure doses, represented in the legend of the graph by the average template CD at each dose. The typical 3σ placement accuracy which was found is 2.7 nm. This value did not show a clear dependency on the template size, apart for a slight increase for the larger template sizes (when the DSA hole is in a way less confined by the walls).

3.3 CD and Placement Accuracy for Doublet DSA Holes

While the above sections 3.1 and 3.2 report on single hole DSA features, this section deals with doublet DSA holes within an

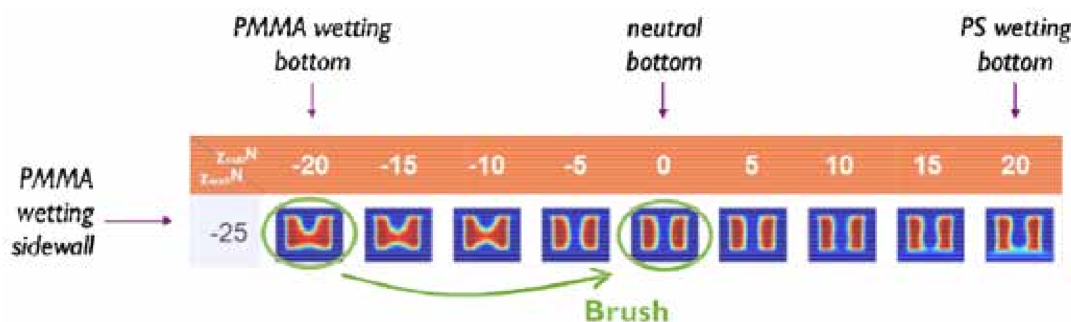

Figure 8. Modeled impacted of the effect that the surface energy of the template bottom has on the DSA hole formation. Courtesy of H. Yi, Stanford University.[6]

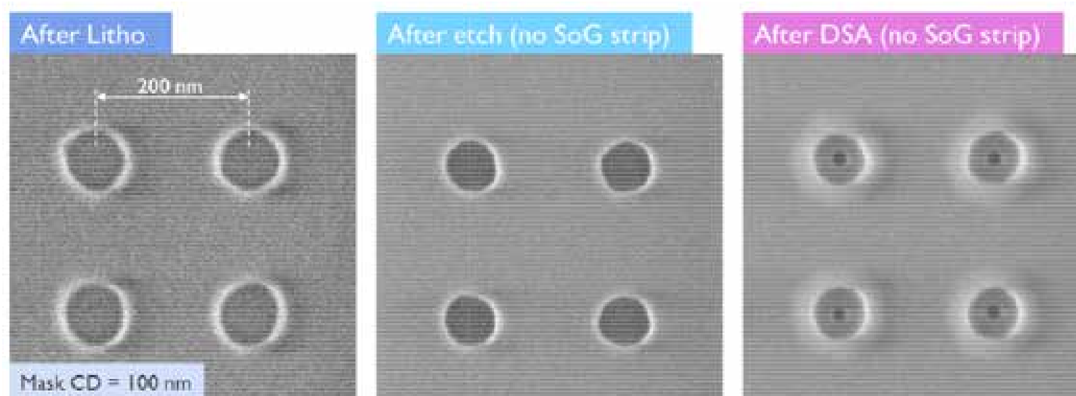

Figure 9. Left to right: templates after litho, after etch, and after DSA application resulting in one DSA hole per template.

elongated template. Given the two DSA holes, we can measure their average CD, and their center-to-center distance referred to as 'DSA pitch' (knowing that the unconstrained BCP pitch of our material is 37 nm). The measured DSA CD and DSA pitch are plotted in Figure 12, as a function of the template X-CD. As for the single DSA holes in section 3.1, the DSA hole CD is found to scale linearly with the template CD. The measured DSA pitch also scales linearly with the template CD, and ranges from 35 to 41 nm. This range shows that some flexibility exists in the DSA pitch, which is not hard fixed to 37 nm. Slight compression or stretch of the hole to hole distance is therefore possible by tuning the template size, but goes along with a small decrease or increase in the DSA hole CD.

As for placement accuracy of the DSA hole doublet within it template, we found a variation of 4.6 nm 3s in the X-direction, and 2.9 nm in Y-direction. This is the variation in center position of the left hole of the doublet with respect to the center of the template. Note that the value for X-direction is larger since the template is less confining in that direction, providing somewhat more freedom for the DSA hole position along X. Also note that the value of 2.9 nm in the Y-direction is very close to the 2.7 nm that was found for the single holes. Indeed, for the doublet, the confinement in the Y-direction resembles that of the single hole. As for the single DSA holes, we saw that these numbers have only minor dependency on the template size.

The variation on the measured DSA pitch was found to be 6.5 nm (slightly lowered to 6.3 nm upon subtracting the template CD correlation). Note that the placement accuracy numbers are still somewhat at the high side, but with further improvements in the DSA flow and in the template patterning, we expect that these numbers can be reduced. Concerning the template patterning, a better fidelity may need to be obtained by means of EUV lithography. Of course, the latter only makes sense as long as the DSA resolution is below that of direct EUV hole patterning.

4. Conclusions and Key Challenges

The imec process for template DSA has been demonstrated. It employs an SoC/SoG/negative tone resist tri-layer stack for template patterning. The templates are demonstrated to be near ideal in terms of their sidewall angle performance. Templated DSA within these pre-patterns is demonstrated using a 37 nm center-to-center BCP material. With very good open hole rate, it has been demonstrated that stable DSA hole patterns can be achieved. Several process options and their impact on the DSA hole formation have been demonstrated.

From latter investigations, we define the key challenges for the implementation of template DSA holes as follows:

- Defectivity control; i.e. missing or excess DSA holes, but also opening of the DSA holes down to the substrate.
- Pattern placement control, both in terms of accuracy and uniformity. As this is linked to the shape definition and the uniformity of the prepattern, it may lead to the need for EUV lithography to create the prepattern. Obviously, this plan only makes sense as long as the DSA pitches are below the resolution limit of EUV.
- Control of the density effects, which have appeared highly

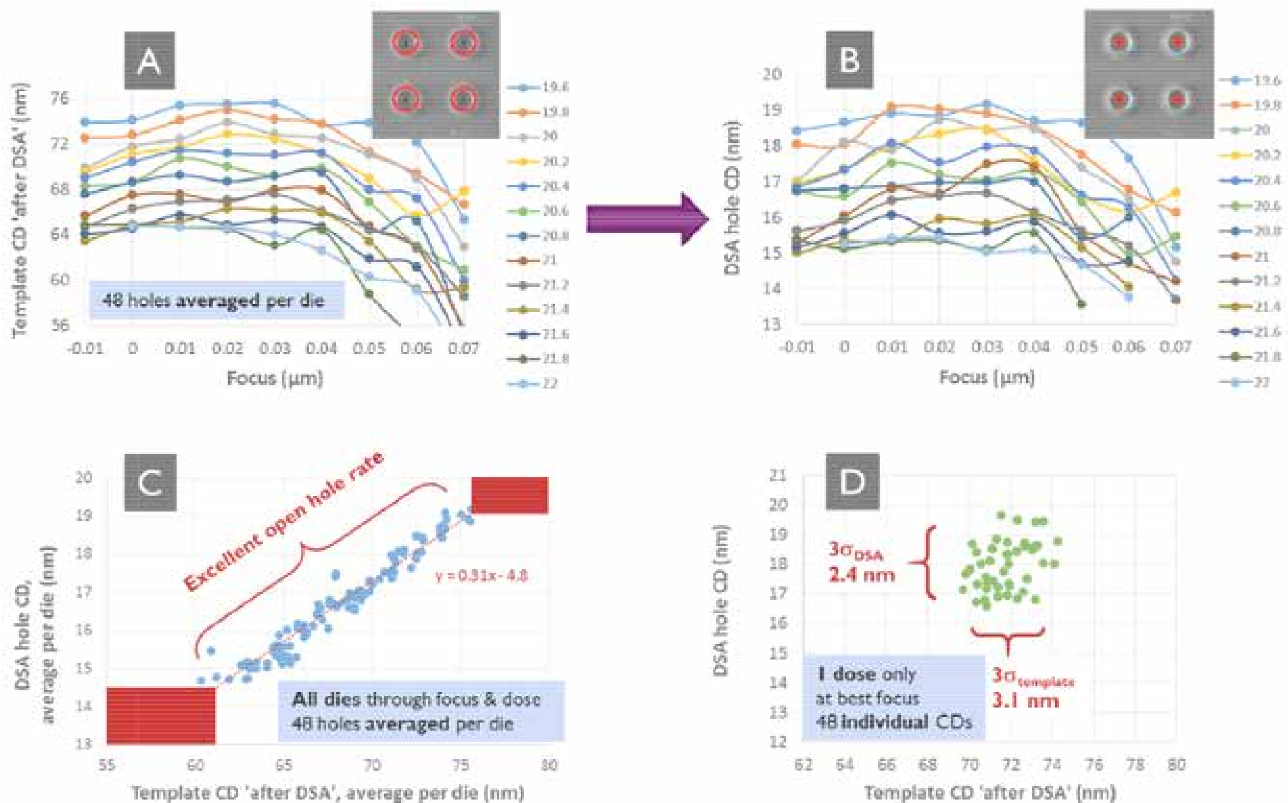

Figure 10. A) Bossung curve of the template CD. B) Corresponding Bossung curve of the DSA hole CD. C) Correlation plot of DSA hole CD versus template CD indicating range of open holes. D) Same correlation without averaging, for one dose at best focus, and indication of 3σ variation on template and DSA hole CDs.

sensitive to process choices. Potentially, the design needs to be adjusted in such was that it is DSA-friendly, in the sense that the density does not span a wide range to avoid over- or underfilling. Alternatively, assisting features that are sub-resolution to DSA-hole formation can be patterned in between the templates to locally capture excess BCP material.

- Surface energy is gating to all points above; a good control helps in the DSA hole fidelity towards the substrate, and in the DSA pattern stability reflecting in improved CD, placement, and process window control.

Essential 'tooling' to be developed soon for the DSA assessment are amongst other improved 3D analysis approaches, as well as top-down SEM metrology algorithms, including contour extraction, dedicated for application on DSA. In addition, the pattern transfer into underlying hard masks needs to be further optimized.

Finally, data has been provided for CD and placement accuracy of DSA holes within 'simple' templates, i.e. single and doublet DSA holes. For these, a very good open hole rate was found, with the disclaimer that only one pattern density was considered for both.

5. Acknowlegments

The authors wish to acknowledge Nadia Vandenbroeck, Jeroen Vandekerkhove, and Frank Holsteins from imec, Safak Sayan from Intel, Doni Parnell and Ainhoa Romo Negreira from Tokyo Electon, and Daisuke Fuchimoto, Kei Sakai and Takashi Ishizawa from Hitachi High Technologies for valuable discussions.

6. References

[1] A. Torres, K. Sakajiri, Y. Granik, Y. Ma, P. Krasnova, S. Nagahara, S. Kawakami, B. Rathsack, G. Khaira, J. de Pablo, and J. Ryckaert, **Proc. SPIE 9052,** (2014) 9052-27.

[2] H.-S. Wong, C. Bencher, H. Yi, X.-Y. Bao, and L.-W. Chang, **Proc. SPIE 8323** (2012) 832303.

[3] Y. Borodovsky, *Semicon West 2012,* June 11, 2012, San Francisco, CA, USA.

[4] R. Gronheid, P. Rincon Delgadillo, A. Singh, T. R. Younkin, S. Sayan, B. T. Chan, L. Van Look, J. Bekaert, I. Pollentier, and P. F. Nealey, *J. Photopolym. Sci. Technol.* 26 (2013) 779.

[5] R. Gronheid, J. Bekaert, V.-K. M. Kuppuswamy, N. Vandenbroeck, J. Doise, Y. Cao, G. Lin, S. Safak, D. Parnell, and M. Somervell, **Proc. SPIE 9051,** (2014) 9051-17.

[6] H. Yi, A. Latypov, and H.-S. Philip Wong, **Proc. SPIE 8680,** (2013) 8680-57.

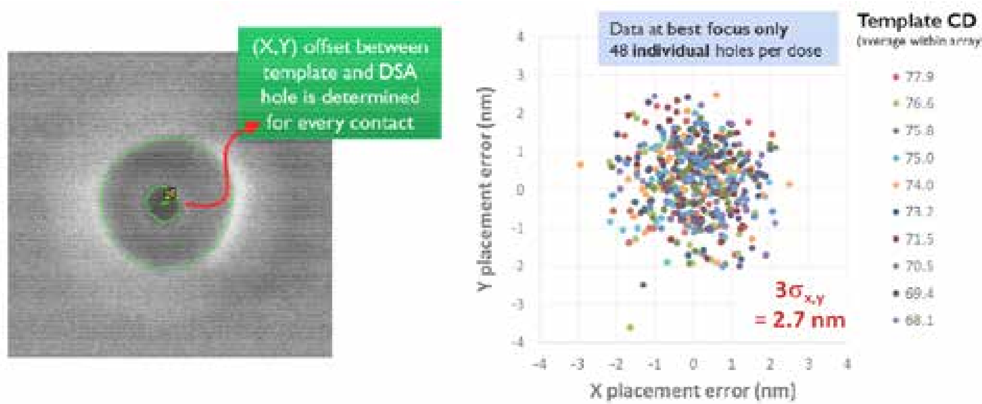

Figure 11. Placement accuracy of the single DSA holes within their template. The graph shows the offset of the center of the DSA hole with respect to the center of the template.

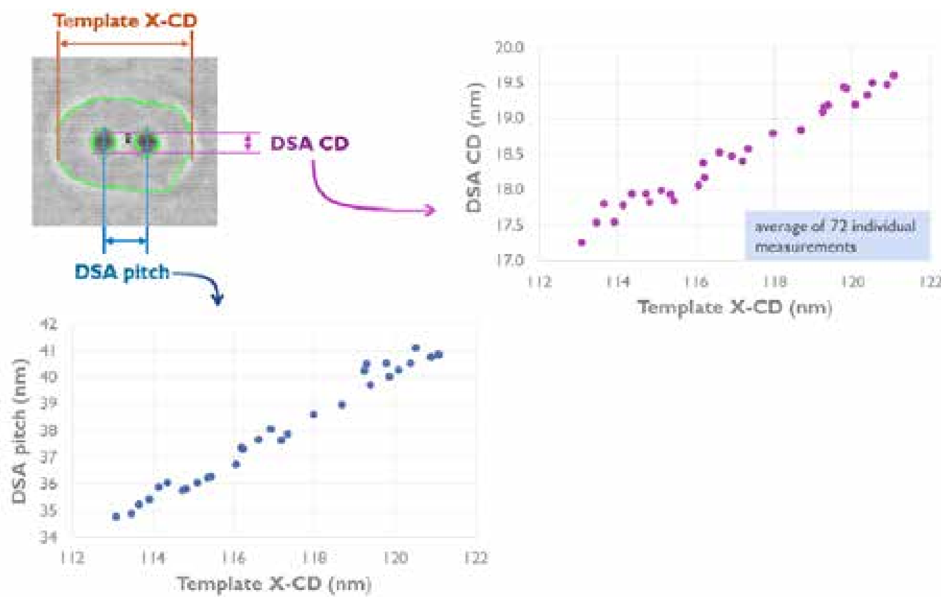

Figure 12. DSA CD and DSA pitch as measured for doublet DSA holes, as function of the template X-CD.

EDITORIAL – *continued from page 3*

- EUV Exposure tools: Mr. van der Horst from ASML showed the Status and roadmap of the NXE:3100 and NXE:3300B platforms. There are 6 NXE:3100 tools at multiple customers qualifying the EUV for the 10 nm logic node. For process development, customers typically require 100 wafers per day, increasing to 500 wafers per day for production qualification. 5 nm overlay is required across the whole wafer over 6 systems and includes effects from projection optics, reticle and wafer clamping.

  Some numbers I wrote down:

	NXE:3100	NXE: 3300B
NA	0.25	0.33
Resolution	27 nm	22 nm
Illumination	Conventional 0.8 s	Conventional 0.9 s 6 off-axis pupil settings
Productivity	6 – 60 wafers/hour	55-125 wafers/hour

NXE technology should be extendable to <7nm.

Technical Exhibition

In parallel with the Conference Presentations, a Technical Exhibition took place where mask, material and equipment suppliers show their companies and products. The exhibition area was also the place for the coffee and lunch breaks.

Next year conference, EMLC2015:

The EMLC2015 will take place in June next year at the Pullman Hotel in Eindhoven, the Netherands, organized by the VDE/GMM in cooperation with ASML.

Sponsorship Opportunities

Sign up now for the best sponsorship opportunities

Photomask 2014 —
Contact: Lara Miles, Tel: +1 360 676 3290; laram@spie.org

Advanced Lithography 2015 —
Contact: Teresa Roles-Meier, Tel: +1 360 676 3290; teresar@spie.org

Advertise in the BACUS News!

The BACUS Newsletter is the premier publication serving the photomask industry. For information on how to advertise, contact:

Lara Miles
Tel: +1 360 676 3290
laram@spie.org

BACUS Corporate Members

Acuphase Inc.
American Coating Technologies LLC
AMETEK Precitech, Inc.
Berliner Glas KGaA Herbert Kubatz GmbH & Co.
FUJIFILM Electronic Materials U.S.A., Inc.
Gudeng Precision Industrial Co., Ltd.
Halocarbon Products
HamaTech APE GmbH & Co. KG
Hitachi High Technologies America, Inc.
JEOL USA Inc.
Mentor Graphics Corp.
Molecular Imprints, Inc.
Panavision Federal Systems, LLC
Profilocolore Srl
Raytheon ELCAN Optical Technologies
XYALIS

Industry Briefs

Mask Blank Inspection Tools for 14nm and 7 nm HP Technology Nodes

ASM International

Lasertec Corp. is introducing MAGICS series M8350/M8351, a new line of mask blank inspection systems that meet the requirements of next-generation photomasks at the technology nodes of 14nm through 7nm. Newest in MAGICS series is designed to meet next-generation inspection needs with high sensitivity suitable for such applications as inspection of quartz substrates for high-end blanks, inspection at various deposition processes, and inspection of resist-coated blanks. M8350/51 has enhanced sensitivity by featuring a new 355nm laser light source as well as by incorporating state-of-the art inspection optics and detection circuitry. With maximum sensitivity of 35nm, M8350/51 has a significantly higher defect detection capability than previous models. Lasertec plans to deliver multiple units in 2014.

ZEISS Launches Next Generation AIMS System

Business Wire

ZEISS introduced the next generation of photomask qualification system AIMS™ 1x-193i at this year´s European Mask and Lithography Conference (EMLC) in Dresden.The new system supports further extension of 193nm lithography and meets the challenging requirements of advanced lithography techniques such as Multi-Patterning and Source Mask Optimization.

AIMS™ enables the user to qualify the optical performance of a mask under scanner equivalent illumination conditions. The AIMS™ 1x-193i works with 193nm illumination and benefits from a completely redesigned optical system. By utilizing FlexIllu® it provides the highest level of illumination flexibility as it is able to read the scanner files for illumination under computer control. Thanks to the advances in the optical design as well as major improvements in the software, the AIMS™ 1x-193i achieves significantly reduced turnaround-times. The enhanced pupil uniformity realizes best scanner and tool-to-tool matching. The first tool has achieved excellent results during customer acceptance procedure and was shipped to their facility.

Mapper Opens Russian MEMS Fab

EE Times

The creation of production facility follows on a 2012 announcement that Russia's Rusnano would invest about €40 million (about $50 million) in Mapper. Rusnano is a government owned investment fund aimed at commercializing developments in nanotechnology. One condition of the Mapper investment was that part of the research and manufacturing in Delft would move to Russia. The MEMS factory is located in Technopolis in Moscow and will have the capacity to produce enough lens elements for the 20 Mapper lithography machines per year, according to Rusnano. Mapper has invested 1 billion rubles (about $30 million) in creating the wafer fab.

It is intended to produce three types of electronic optics at the Moscow plant. The simplest of them are spacers, which are used to separate electronic optical elements. Next in the order of complexity are silicon electronic lenses for focusing and collimation of electron beams. They will come into production by the end of 2014. Production of the most complex elements, containing electronics for control electrodes, is scheduled to begin by the end of 2015.

Join the premier professional organization for mask makers and mask users!

About the BACUS Group

Founded in 1980 by a group of chrome blank users wanting a single voice to interact with suppliers, BACUS has grown to become the largest and most widely known forum for the exchange of technical information of interest to photomask and reticle makers. BACUS joined SPIE in January of 1991 to expand the exchange of information with mask makers around the world.

The group sponsors an informative monthly meeting and newsletter, BACUS News. The BACUS annual Photomask Technology Symposium covers photomask technology, photomask processes, lithography, materials and resists, phase shift masks, inspection and repair, metrology, and quality and manufacturing management.

Individual Membership Benefits include:

- Subscription to BACUS News (monthly)
- Eligibility to hold office on BACUS Steering Committee

www.spie.org/bacushome

Corporate Membership Benefits include:

- 3-10 Voting Members in the SPIE General Membership, depending on tier level
- Subscription to BACUS News (monthly)
- One online SPIE Journal Subscription
- Listed as a Corporate Member in the BACUS Monthly Newsletter

www.spie.org/bacushome

Calendar

2014

SPIE Photomask Technology

Co-located with
SPIE Scanning Microscopies

16-18 September 2014
Monterey Marriott and
Monterey Conference Center
Monterey, California, USA
www.spie.org/pm

SPIE Scanning Microscopies

Co-located with
SPIE Photomask Technology

16-18 September 2014
Monterey Marriott and
Monterey Conference Center
Monterey, California, USA
www.spie.org/sg

2015

SPIE Advanced Lithography
22-26 February 2015
San Jose Convention Center
and San Jose Marriott
San Jose, California, USA
www.spie.org/al

SPIE is the international society for optics and photonics, a not-for-profit organization founded in 1955 to advance light-based technologies. The Society serves nearly 225,000 constituents from approximately 150 countries, offering conferences, continuing education, books, journals, and a digital library in support of interdisciplinary information exchange, professional growth, and patent precedent. SPIE provided over $3.2 million in support of education and outreach programs in 2013.

SPIE.

International Headquarters
P.O. Box 10, Bellingham, WA 98227-0010 USA
Tel: +1 360 676 3290
Fax: +1 360 647 1445
help@spie.org • www.SPIE.org

Shipping Address
1000 20th St., Bellingham, WA 98225-6705 USA

Managed by SPIE Europe
2 Alexandra Gate, Ffordd Pengam, Cardiff,
CF24 2SA, UK
Tel: +44 29 2089 4747
Fax: +44 29 2089 4750
spieeurope@spieeurope.org • www.spieeurope.org

You are invited to submit events of interest for this calendar. Please send to lindad@spie.org; alternatively, email or fax to SPIE.